

# Adversarial $\alpha$ -divergence Minimization for Bayesian Approximate Inference

Simón Rodríguez Santana<sup>a,\*</sup>, Daniel Hernández-Lobato<sup>b</sup>

<sup>a</sup>*Institute of Mathematical Sciences (ICMAT-CSIC), Campus de Cantoblanco, C/Nicolás Cabrera, 13-15, 28049 Madrid, Spain.*

<sup>b</sup>*Escuela Politécnica Superior, Universidad Autónoma de Madrid, Campus de Cantoblanco, C/Francisco Tomás y Valiente 11, 28049 Madrid, Spain.*

---

## Abstract

Neural networks are popular models for regression. They are often trained via back-propagation to find a value of the weights that correctly predicts the observed data. Although back-propagation has shown good performance in many applications, it cannot easily output an estimate of the uncertainty in the predictions made. Measuring this uncertainty in the predictions of machine learning models is a critical aspect with important applications. Uncertainty estimates can be obtained by following a Bayesian approach in which a posterior distribution of the model parameters is computed. The posterior distribution summarizes which parameter values are compatible with the data. Typically, this posterior distribution is intractable and has to be approximated. Several approaches have been considered for solving this problem. We propose here a general method for approximate Bayesian inference based on minimizing  $\alpha$ -divergences which allows for flexible approximate distributions. The method is evaluated in the context of Bayesian neural networks for regression on extensive experiments. The results show that it often gives better performance in terms of the test log-likelihood and sometimes in terms of the squared error.

*Keywords:* Bayesian Neural Networks, Approximate Inference, Alpha Divergences, Adversarial Variational Bayes

---

\*Corresponding author

*Email addresses:* `simon.rodriguez@icmat.es` (Simón Rodríguez Santana ),  
`daniel.hernandez@uam.es` (Daniel Hernández-Lobato)

## 1. Introduction

In the past years, Neural Networks (NNs) have become very popular due to the empirical achievements in a wide variety of problems. Specifically, Deep Neural Networks (DNNs) trained with back-propagation have significantly improved the state-of-the-art in supervised learning tasks [1]. Moreover, variations of the simple original NN models have been specifically designed to take advantage of underlying structure on the input data. This is the case for Convolutional Neural Networks (CNNs) [2] or Long-Short Term Memory Networks (LSTMs) [3], both of which represent some of the best performing models for dealing with structured data such as images and texts, respectively. NNs can be trained on Graphical Processing Units (GPUs), which significantly reduces the total training time and the effort needed to produce highly accurate results. These models can therefore be trained on huge amounts of data very quickly, showing excellent results both in regression and in classification tasks.

In spite of the advantages described, the good performance results come with some drawbacks, such as the concerns about over-fitting due to the high number of parameters to be adjusted, or the lack of a confidence measure on the predicted outputs associated to the input data [4]. More precisely, regular NNs only produce point-estimate predictions and do not provide any information about the certainty of such outcome. Even in multi-class problems where the results are given in terms of a soft-max function which outputs probabilities, it is important to keep in mind that the output values do not correspond to the confidence of the prediction. In particular, a high class label probability may correspond to a data instance that will be often misclassified by the network.

The problems described can be easily addressed by following a Bayesian approach in the training process, instead of relying on back-propagation for finding point-estimates of the model parameters. Bayesian probabilistic models such as Bayesian neural networks (BNNs) [5] can capture the uncertainty in the model parameters (the network weights) and the effects it produces in the final predictions, therefore providing an estimate of the models' ignorance on

the input data in each specific case. This extra output information can be used in different ways. For example, to confront problems in artificial intelligence safety, perform active learning, or to deal with possible adversaries which may manipulate the data [4]. Summing up, uncertainty estimates associated to the model predictions are very important to make optimal decisions when dealing with input data that the machine learning algorithm has never seen before.

The Bayesian approach relies on computing a posterior distribution for the model parameters given the observed data [4]. This posterior distribution is obtained using Bayes' rule simply by multiplying a likelihood function (which captures how well specific values of the parameters explain the observed data) and a prior distribution (which includes prior knowledge about what potential values this parameters may take). This posterior distribution summarizes which model parameters (*i.e.*, the neural network weights) are compatible with the observed data. Intuitively, if the model is rather complex, the posterior will be very broad. By contrast, if the model is fairly simple, the posterior will concentrate on a specific region of the parameters space. The information contained in the posterior distribution can be readily translated into a predictive distribution which carries information about the uncertainty on the predictions made. For this, one simply has to average the predictions of the model for each parameter configuration weighted by the corresponding posterior probability.

A difficulty of the Bayesian approach is, however, that computing the posterior distribution is intractable for most problems. Therefore, in practice, one has to resort to approximate methods. Most of these methods approximate the exact posterior using a distribution  $q$ . The parameters of  $q$  are tuned by minimizing a divergence between  $q$  and the exact posterior. This is how methods such as variational inference (VI), expectation propagation (EP) or black-box-alpha work in practice [6, 7, 8]. Although this methods are very fast and scalable, a limitation is the lack of flexibility of the approximate distribution  $q$ , which is often set to be a parametric distribution that cannot adequately match the exact posterior. Therefore, these methods suffer from strong approximation bias. Importantly, a poor approximation of the exact posterior is expected to lead to

a worse predictive distribution, less accurate predictions, and a worse estimate of the uncertainty in the predictions made.

Recently, several methods have been proposed to increase the flexibility of the approximate distribution  $q$  [9, 10, 11, 12]. Among these, a successful approach is to use an implicit model for the approximate distribution  $q$  [13]. Under this setting,  $q$  is simply obtained by applying an adjustable non-linear function (*e.g.*, given by the output of a neural network) to a source of Gaussian noise. If the non-linear function is flexible enough, almost any distribution can be approximated like this. The problem is, however, that even though  $q$  is a distribution that is easy to sample from, its p.d.f. can not be obtained analytically due to the complexity of the non-linear function. This makes approximate inference (*i.e.*, tuning the parameters of the non-linear function) very challenging. Adversarial variational Bayes (AVB) is a technique that solves this problem [10]. AVB minimizes the Kullback-Leibler (KL) divergence between  $q$  and the exact posterior. This technique avoids evaluating the p.d.f. of  $q$  by learning a discriminator network that estimates the log-ratio between  $q$  and the prior distribution over the model parameters.

AVB and also other methods such as VI or EP (only locally and in the reversed way) rely on minimizing the KL divergence between the approximate distribution  $q$  and the exact posterior. The  $\alpha$ -divergence generalizes the KL divergence and includes a parameter  $\alpha \in (0, 1]$  that can be adjusted. In particular, when  $\alpha \rightarrow 0$ , the  $\alpha$ -divergence tends to the KL-divergence optimized by VI. By contrast, if  $\alpha = 1$ , the  $\alpha$ -divergence is the reversed KL-divergence, *i.e.*, the KL-divergence between the exact posterior and  $q$ , which is locally optimized by EP. Recently, it has been empirically shown that one can obtain better results in terms of the approximate predictive distribution by minimizing  $\alpha$ -divergences locally using intermediate values of the  $\alpha$  parameter, in the case of parametric  $q$  [7]. It is not clear however if one can also obtain better results in the case of implicit models for  $q$ , such as the one considered by AVB.

In this paper we extend AVB to locally minimize  $\alpha$ -divergences, in an approximate way, instead of the regular KL divergence, being  $\alpha$  a parameter.

Therefore, this method can be seen as a generalization of AVB that allows to optimize a more general class of divergences, resulting in flexible approximate distributions  $q$  with different properties. When  $\alpha \rightarrow 0$ , the proposed method converges to standard AVB. When  $\alpha = 1$  the proposed method is similar to EP with a flexible approximate distribution  $q$ . We have evaluated such a method in the context of Bayesian Neural Networks and tested different values of the  $\alpha$  parameter. The experiments carried out (involving several regression problems extracted from the UCI repository) show that one can obtain better prediction results than those of AVB and standard VI, in terms of the mean squared error and the test log-likelihood, by using intermediate values of  $\alpha$ .

## 2. Variational Inference and Adversarial Variational Bayes

Adversarial Variational Bayes (AVB) is an extension of variational inference (VI) [14] that allows for implicit models for the approximate distribution  $q$ . We describe here first VI and then AVB in detail.

### 2.1. Variational Inference

Let  $\mathbf{w}$  be the latent variables of the model, *e.g.*, the neural network weights. The task of interest in VI is to approximate the posterior distribution of  $\mathbf{w}$  given the observed data. For simplicity we will focus on regression models, but the method is broadly applicable to any model and is not limited to neural networks.

Consider a training set  $\mathcal{D} = \{\mathbf{x}_i, y_i\}_{i=1}^N$ , where  $\mathbf{x}_i$  is some  $d$ -dimensional input vectors and  $y_i \in \mathbb{R}$  is the associated label. The posterior distribution is given by Bayes' rule:

$$p(\mathbf{w}|\mathcal{D}) = \frac{p(\mathbf{y}|\mathbf{w}, \mathbf{X})p(\mathbf{w})}{p(\mathcal{D})} = \frac{\left[ \prod_{i=1}^N p(y_i|\mathbf{w}, \mathbf{x}_i) \right] p(\mathbf{w})}{p(\mathcal{D})}, \quad (1)$$

where  $\mathbf{X}$  is a matrix with the observed vectors of input attributes and  $\mathbf{y} = (y_1, \dots, y_N)^T$ . Furthermore we have assumed i.i.d. data and hence, the likelihood factorizes as  $p(\mathbf{y}|\mathbf{w}, \mathbf{X}) = \prod_{i=1}^N p(y_i|\mathbf{w}, \mathbf{x}_i)$ . In (1)  $p(\mathbf{w})$  is the prior distribution of the latent variables of the model (*i.e.*, the neural network weights) and

$p(\mathcal{D}) = \int p(\mathbf{y}|\mathbf{w}, \mathbf{X})p(\mathbf{w})d\mathbf{w}$  is just a normalization constant. In the case of regression problems  $p(y_i|\mathbf{w}, \mathbf{x}_i)$  is often a Gaussian distribution, *i.e.*,  $\mathcal{N}(y_i|f(\mathbf{x}_i), \sigma^2)$ , where  $f(\mathbf{x}_i)$  is the output of the neural network and  $\sigma^2$  is the variance of the output noise. Furthermore,  $p(\mathbf{w})$  is often a factorizing Gaussian with zero mean and variance  $\sigma_0^2$  (see *e.g.*, [6, 8, 7]). Given (1) the predictive distribution of the model for the label  $y^*$  of a new test point  $\mathbf{x}_*$  is:

$$p(y^*|\mathcal{D}) = \int p(y^*|\mathbf{w}, \mathbf{x}_*)p(\mathbf{w}|\mathcal{D})d\mathbf{w}. \quad (2)$$

The model prediction would be the expected value of  $y^*$  under (2) and the confidence in the prediction can be estimated, *e.g.*, by the standard deviation. In practice,  $p(\mathbf{w}|\mathcal{D})$  is intractable because  $p(\mathcal{D})$  has no closed form expression and one has to use an approximation to this distribution in (2).

VI approximates (1) using a parametric distribution  $q(\mathbf{w})$  which is often a factorizing Gaussian  $\mathcal{N}(\mathbf{w}|\boldsymbol{\mu}, \boldsymbol{\Sigma})$  with  $\boldsymbol{\Sigma}$  a diagonal matrix. Let  $\phi$  be the set of parameters of  $q$ , *i.e.*,  $\phi = \{\boldsymbol{\mu}, \boldsymbol{\Sigma}\}$ . These parameters are adjusted to minimize the KL divergence between  $q$  and the exact posterior (1). Consider the following decomposition of  $\log p(\mathcal{D})$ :

$$\log p(\mathcal{D}) = \mathbb{E}_{q_\phi(\mathbf{w})}[\log p(\mathbf{y}, \mathbf{w}|\mathbf{X})] + \text{KL}(q|p), \quad (3)$$

where  $\text{KL}(q|p)$  is the KL divergence between  $q$  and the exact posterior:

$$\text{KL}(q|p) = - \int q_\phi(\mathbf{w}) \log \frac{p(\mathbf{w}|\mathcal{D})}{q_\phi(\mathbf{w})} d\mathbf{w} \geq 0. \quad (4)$$

The KL divergence is always non-negative and is only equal if the two distributions are the same. Therefore, by minimizing this divergence VI enforces that  $q$  looks similar to the exact posterior (1).

Because  $\log p(\mathcal{D})$  is a constant term independent of  $\phi$ , the KL divergence between  $q$  and the exact posterior can be simply minimized by maximizing the first term in the r.h.s. of (3) with respect to  $\phi$ . This term is often referred to

as the evidence lower bound:

$$\mathcal{L}(\phi) = \mathbb{E}_{q_\phi(\mathbf{w})}[\log p(\mathbf{y}, \mathbf{w}|\mathbf{X})] = \sum_{i=1}^N \mathbb{E}_{q_\phi(\mathbf{w})}[p(y_i|\mathbf{w}, \mathbf{x}_i)] - \text{KL}(q|\text{prior}), \quad (5)$$

where  $\text{KL}(q|\text{prior})$  is the KL divergence between  $q$  and the prior  $p(\mathbf{w})$ . If  $q$  and the prior are Gaussian, there is a closed form expression for this divergence. The maximization of (5) can be done using stochastic optimization techniques that sub-sample the training data and that approximate the required expectations using Monte Carlo samples. See [8] for further details. The hyper-parameters of the model, *i.e.*, the noise and prior variance  $\sigma^2$  and  $\sigma_0^2$  are estimated by maximizing  $\mathcal{L}(\phi)$ , which approximates  $\log p(\mathcal{D})$  since  $\text{KL}(q|p)$  is expected to be fairly small. Finally, after training, the posterior approximation can replace the exact posterior in (2) and the predictive distribution for new data can be approximated by a Monte Carlo average over the posterior samples.

## 2.2. Adversarial Variational Bayes

AVB extends VI to account for implicit models for the approximate distribution  $q$ . An implicit model for  $q$  is a distribution that is easy to generate samples from, but that lacks a closed form expression for the p.d.f. An example is a source of standard Gaussian noise that is non-linearly transformed by a neural network. That is,

$$q_\phi(\mathbf{w}) = \int \delta(\mathbf{w} - \mathbf{f}_\phi(\boldsymbol{\epsilon})) \mathcal{N}(\boldsymbol{\epsilon}|\mathbf{0}, \mathbf{I}) d\boldsymbol{\epsilon}, \quad (6)$$

where  $\mathbf{f}_\phi(\boldsymbol{\epsilon})$  is the output of a neural network that receives  $\boldsymbol{\epsilon}$  at the input and  $\delta(\cdot)$  is a delta function. In general, the integral in (6) is intractable due to the strong non-linearities of the neural network. Nevertheless, it is very easy to generate  $\mathbf{w} \sim q_\phi$ . For this, one only has to generate  $\boldsymbol{\epsilon} \sim \mathcal{N}(\mathbf{0}, \mathbf{I})$  to then compute  $\mathbf{w} = \mathbf{f}_\phi(\boldsymbol{\epsilon})$ . If the noise dimension is large enough and  $\mathbf{f}_\phi(\cdot)$  is flexible enough, any probability distribution can be described like this. Therefore, implicit models can alleviate the approximation bias of VI with parametric distributions  $q$ .

Using an implicit distribution in VI is challenging because the lower bound in (5) cannot be easily evaluated nor optimized. The reason is that the term  $\text{KL}(q|\text{prior})$ , *i.e.*, the KL divergence between the approximate distribution  $q$  and the prior requires the p.d.f. of  $q$ . AVB provides an elegant solution to this problem. The aforementioned term can be written as:

$$\text{KL}(q|\text{prior}) = \mathbb{E}_{q_\phi(\mathbf{w})} [\log q_\phi(\mathbf{w}) - \log p(\mathbf{w})] = \mathbb{E}_{q_\phi(\mathbf{w})} [T(\mathbf{w})], \quad (7)$$

where  $T(\mathbf{w})$  is simply the log-ratio between  $q_\phi$  and the prior. AVB proposes to estimate this log-ratio as the output of another neural network that discriminates between samples of  $\mathbf{w}$  generated from  $q_\phi$  and from the prior [10]. Let  $T_\omega(\cdot)$  be the output of the discriminator. The following objective is considered for optimizing the discriminator assuming  $q_\phi(\mathbf{w})$  is fixed:

$$\max_{\omega} \mathbb{E}_{q_\phi(\mathbf{w})} \log \sigma(T_\omega(\mathbf{w})) + \mathbb{E}_{p(\mathbf{w})} \log(1 - \sigma(T_\omega(\mathbf{w}))), \quad (8)$$

where  $\sigma(\cdot)$  is the sigmoid-function. Roughly speaking, this objective tries to make the discriminator differentiate between samples generated from  $q_\phi(\mathbf{w})$  and from the prior  $p(\mathbf{w})$ .

If the discriminator  $T_\omega$  is considered flexible enough to represent any function of  $\mathbf{w}$ , it is possible to prove that the optimal discriminator behaves as expected. If we rewrite (8) we obtain

$$\max_{\omega} \int [q_\phi(\mathbf{w}) \log \sigma(T_\omega(\mathbf{w})) + p(\mathbf{w}) \log(1 - \sigma(T_\omega(\mathbf{w})))] d\mathbf{w}. \quad (9)$$

This integral is maximal for  $T_\omega(\mathbf{w})$  if and only if the integrand is maximal for every  $\mathbf{w}$  value. The shape of the integrand is:

$$a \log t + b \log(1 - t), \quad (10)$$

for  $a = q_\phi(\mathbf{w})$ ,  $b = p(\mathbf{w})$ , and  $t = T_\omega(\mathbf{w})$ . Its maximum value is attained at

$t = \frac{a}{a+b}$ . Therefore, the optimal solution  $T_{\omega^*}$  is

$$\sigma(T_{\omega^*}(\mathbf{w})) = \frac{q_\phi(\mathbf{w})}{q_\phi(\mathbf{w}) + p(\mathbf{w})}, \quad (11)$$

or equivalently,

$$T_{\omega^*}(\mathbf{w}) = \log q_\phi(\mathbf{w}) - \log p(\mathbf{w}). \quad (12)$$

which is the result desired to correctly estimate the KL divergence between  $q_\phi$  and the prior. In particular, the discriminator can be plugged in (7) and the expectation can be approximated simply by a Monte Carlo average by generating samples from  $q_\phi$ .

Given  $T_{\omega^*}$  the lower bound employed in AVB is obtained by re-writing the evaluation of the KL divergence between  $q_\phi$  and the prior:

$$\mathcal{L}(\phi) = \sum_{i=1}^N \mathbb{E}_{q_\phi(\mathbf{w})} [p(y_i | \mathbf{w}, \mathbf{x}_i)] - \mathbb{E}_{q_\phi(\mathbf{w})} [T_{\omega^*}(\mathbf{w})]. \quad (13)$$

Note that all the required expectations can be simply approximated by generating samples from  $q_\phi$  and the sum across the training data can be approximated using a mini-batch. This lower bound can be hence easily maximized w.r.t.  $\phi$  using stochastic optimization techniques. For this, however, we need to differentiate the stochastic estimate with respect to  $\phi$ . This may seem complicated since  $T_{\omega^*}(\mathbf{w})$  is defined as the solution of an auxiliary optimization problem that depends on  $\phi$ . However, due to the expression for the optimal discriminator, it can be showed that  $\mathbb{E}_{q_\phi(\mathbf{w})} (\nabla_\phi T_{\omega^*}(\mathbf{w})) = 0$ . Therefore the dependence of  $T_{\omega^*}(\mathbf{w})$  w.r.t  $\phi$  can be ignored. See [10] for further details. In practice, both  $q_\phi$  and the discriminator  $T_\omega(\mathbf{w})$  are trained simultaneously. However,  $q_\phi$  is updated by maximizing (13) using a smaller learning rate than the one used to update the discriminator  $T_\omega$ , which considers the objective in (8). This guarantees that  $T_\omega$  is an accurate estimator of the log-ratio between  $q_\phi$  and the prior, and that the KL divergence is correctly estimated when updating  $q_\phi$ .

### 2.3. Adaptive Contrast

AVB relies on a good approximation  $T_\omega(\mathbf{w})$  to the optimal discriminator. Although in the non-parametric limit this is achieved, in practice  $T_\omega(\mathbf{w})$  can fail to be sufficiently close to the optimal discriminator. This is a consequence of AVB calculating the discriminator between  $q_\phi$ , the posterior approximation and the prior, which are often very different distributions. This results in practice in a more *relaxed* performance of the estimated discriminator, which has no problem telling apart samples from one density or the other, but that fails to correctly estimate the log-ratio between probability distributions.

In [10] a solution is proposed, which consists in introducing a new auxiliary conditional probability distribution  $r_\alpha(\mathbf{w})$  with known density that approximates  $q_\phi$ . This auxiliary distribution is set to be a factorizing Gaussian whose mean and variances match those of  $q_\phi$ . Using this extra distribution, the objective in (5) is rewritten as

$$\mathcal{L}(\phi) = -\text{KL}(q_\phi|r_\alpha) + \mathbb{E}_{q_\phi(\mathbf{w})} [\log p(\mathbf{y}|\mathbf{w}, \mathbf{X}) - \log r_\alpha(\mathbf{w})] . \quad (14)$$

If  $r_\alpha(\mathbf{w})$  approximates well  $q_\phi(\mathbf{w})$ , the KL divergence between these distributions will often be much smaller than  $\text{KL}(q_\phi|\text{prior})$ , which facilitates learning the correct probability ratio.

This technique is called *adaptive contrast*, because the divergence is not being calculated between  $q_\phi$  and the prior, but between  $q_\phi$  and the adaptive distribution  $r_\alpha$ . Therefore, the discriminator now estimates  $\text{KL}(q_\phi|r_\alpha)$  and hence the log-ratio between  $q_\phi$  and  $r_\alpha$ . More precisely, the lower bound becomes

$$\mathcal{L}(\phi) = \mathbb{E}_{q_\phi(\mathbf{w})} [-T_\omega(\mathbf{w}) - \log r_\alpha(\mathbf{w}) + \log p(\mathbf{y}|\mathbf{w}, \mathbf{X})] , \quad (15)$$

where now  $T_\omega(\mathbf{w})$  approximates the optimal discriminator between samples from  $r_\alpha(\mathbf{w})$  and  $q_\phi(\mathbf{w})$ . Moreover, the KL divergence in (14) is invariant under any

change of variables. Therefore, it can be rewritten as:

$$\text{KL}(q_\phi|r_\alpha) = \text{KL}(\tilde{q}_\phi|r_0), \quad (16)$$

where  $\tilde{q}_\phi(\tilde{\mathbf{w}})$  is the distribution of the standardized vector  $\tilde{\mathbf{w}}$ , whose  $j$ -th component is given by  $\tilde{w}_j := \frac{w_j - \mu_j}{\sqrt{\Sigma_{j,j}}}$  (with  $\mu_j$  and  $\Sigma_{j,j}$  the mean and variance of  $w_j$ , respectively), and  $r_0(\tilde{\mathbf{w}})$  is a standard Gaussian distribution. Therefore, the discriminator  $T_\omega(\mathbf{w})$  just needs to look for differences between samples from the normalized posterior approximation and from a standard Gaussian distribution. The mean and variances of  $\mathbf{w}$  under  $q_\phi$  can simply be estimated using samples from this distribution.

### 3. Alpha Divergence Minimization

Before describing the proposed method, we briefly review here the  $\alpha$ -divergence, of which we make extensive use. Let  $p$  and  $q$  be two distributions over the vector  $\boldsymbol{\theta}$ . The  $\alpha$ -divergence between  $p$  and  $q$  is non-negative and only equal to zero if  $p = q$  [15]. The corresponding expression is given by

$$D_\alpha[p|q] = \frac{1}{\alpha(1-\alpha)} \left( 1 - \int p(\boldsymbol{\theta})^\alpha q(\boldsymbol{\theta})^{1-\alpha} d\boldsymbol{\theta} \right). \quad (17)$$

This divergence has a parameter  $\alpha \in \mathbb{R} \setminus \{0, 1\}$ . Depending on the value of  $\alpha$  it recovers different well-known divergences between probability distributions. For example,

$$D_1[p|q] = \lim_{\alpha \rightarrow 1} D_\alpha[p|q] = \text{KL}[p|q], \quad (18)$$

$$D_0[p|q] = \lim_{\alpha \rightarrow 0} D_\alpha[p|q] = \text{KL}[q|p], \quad (19)$$

$$D_{\frac{1}{2}}[p|q] = 2 \int \left( \sqrt{p(\boldsymbol{\theta})} - \sqrt{q(\boldsymbol{\theta})} \right)^2 d\boldsymbol{\theta} = 4\text{Hel}^2[p|q]. \quad (20)$$

The first two limiting cases given by (18) and (19) represent the two different possibilities for the KL-divergence between distributions. Moreover, (20) is

known as the *Hellinger distance*, which is the only instance in the family of  $\alpha$ -divergences which is symmetric between both distributions.

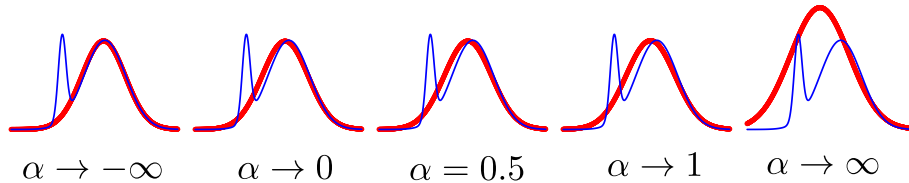


Figure 1: Changes on the approximate distribution  $q$  (in red) when trying to approximate it to the original distribution  $p$  (in blue) using different values for  $\alpha$  in the  $\alpha$ -divergence. When  $\alpha \rightarrow -\infty$  the approximate distribution tries to cover a local mode of the target distribution (*exclusive distribution*). When  $\alpha \rightarrow \infty$  the approximate distribution tries to cover the whole target distribution (*inclusive distribution*). The expression for the  $\alpha$ -divergence can be generalized so that it can be evaluated on distributions that need not be normalized. See [16] for further details.

The value of the  $\alpha$  parameter in the  $\alpha$ -divergence has a strong impact in the inference results. Thus, to further understand its effect lets consider a toy problem in which we try to approximate a *slightly complex* distribution  $p$  with a more simple one,  $q$ . If we considered for example  $p$  as a bimodal distribution and  $q$  as a simple Gaussian distribution we would obtain the results displayed in Figure 1 (reproduced from [16]). In this figure, the resulting (unnormalized) approximating distributions exhibit different behaviors. First of all, in the limit of  $\alpha \rightarrow -\infty$ ,  $q$  (here represented in red) tends to cover only the mode with the larger mass of the two present in  $p$ . By contrast, when  $\alpha \rightarrow \infty$ ,  $q$  tends to cover the whole  $p$  distribution, overlaying the latter completely. This can be seen in terms of the form of the  $\alpha$ -divergence. More precisely, for  $\alpha \leq 0$ , the  $\alpha$ -divergence emphasizes  $q$  to be small whenever  $p$  is small (thus it could be considered as zero-forcing). On the other hand, when  $\alpha \geq 1$ , it can be said that the divergence is inclusive, following the terminology of [17]. In this case, the divergence enforces  $q > 0$  wherever  $p > 0$ , hence avoiding not having probability density in regions of the input space in which  $p$  takes large values.

In rest of the cases,  $\alpha$  lays inside the interval  $(0, 1)$ . The behavior of  $q$  is intermediate between the two extreme possibilities that we have seen so far. In

Figure 1 we can see that when  $\alpha \rightarrow 0$  the  $q$  distribution is more centered in the main mode of  $p$ , whereas in  $\alpha \rightarrow 1$  it begins to open to account for some of the mass of the secondary peak of  $p$ . This type of changes happen also when the distributions being considered are more complex than these ones, and therefore one has to be careful when choosing  $\alpha$ . In particular, the optimal value of  $\alpha$  may depend on the task at hand and the particular model one is working with. As it has been pointed out before, when  $\alpha$  is restricted to be in the interval  $(0, 1)$  we can obtain two notable results at the extremes,  $D_\alpha = \text{KL}(q|p)$  for  $\alpha \rightarrow 0$  and  $D_\alpha = \text{KL}(q|p)$  for  $\alpha \rightarrow 1$ . These two expressions are directly related to two of the main methods for approximate inference, Variational Inference [14] and Expectation Propagation [18], respectively.

#### 4. Adversarial Alpha Divergence Minimization

So far we have seen that AVB is a flexible method for approximate inference that allows for the use of implicit models for the approximate distribution  $q_\phi$ . If the complexity of the implicit model is large enough, AVB should be able to capture important properties of the target distribution. However, AVB strongly relies on the KL divergence to enforce that the approximate distribution looks similar to the target distribution. In Section 3 we have pointed out that by employing a more general form of divergence one can obtain more flexible results, which may balance better between approximating a local mode of the posterior distribution and having high probability density in all the regions of the input space in which the target distribution has high probability. The method proposed is a generalization of AVB that allows for optimizing, in an approximate way, the  $\alpha$ -divergence, instead of the KL divergence. By changing the  $\alpha$  parameter one can hence obtain different approximate distributions  $q$ . We refer to this method as Adversarial Alpha Divergence Minimization. If we are able to use values of  $\alpha$  different to the ones that are used in AVB (*i.e.*,  $\alpha \rightarrow 0$ ) we can perhaps obtain approximating distributions that yield better results in terms of the prediction error or the test log-likelihood.

As discussed earlier, when  $\alpha \rightarrow 0$ , the  $\alpha$ -divergence recovers the KL divergence typical from VI, and when  $\alpha \rightarrow 1$ , the opposite KL divergence is restored (which is the one employed in other algorithms such as Expectation Propagation [18]). We can therefore explore the range of values of  $\alpha$  between 0 and 1 to search for a more suited value for each learning task, and besides this, we can also try to analyze the general behavior of the approximate inference method.

To introduce the use of  $\alpha$ -divergences in the context of AVB we modify the AVB objective function so that it accounts for this extra parameter as well. To do so we follow the approach described in [19], which allows for the approximate minimization of  $\alpha$ -divergences with approximate distributions  $q$  that are not implicit.

#### 4.1. Power Expectation Propagation

We consider the objective function of a general method for approximate inference known as power expectation propagation (PEP) [20]. PEP allows for minimizing  $\alpha$ -divergences in an approximate way, but constrains the approximate distribution  $q$  to belong to the family of exponential distributions (*i.e.*,  $q$  must be a Gaussian distribution). More precisely, the global minimization of the  $\alpha$ -divergence is intractable, except when  $\alpha \rightarrow 0$ . See [16] for further details. Let the target unnormalized distribution be the product of several factors, *i.e.*,  $p \propto \prod_i f_i$ . In general, if we have i.i.d. data, this is always the case, since the likelihood factorizes. PEP approximates  $p$  by  $q$ , which is written as a product of simple factors  $q \propto \prod_i \tilde{f}_i$ , where each  $\tilde{f}_i$  belongs to the exponential family (*i.e.*, it is, *e.g.*, a Gaussian factor) and approximates the corresponding exact factor  $f_i$ . PEP minimizes the  $\alpha$ -divergence locally, instead of globally. In particular, PEP minimizes the  $\alpha$ -divergence between the tilted distributions of the model, and the approximate distribution  $q$ . The tilted distributions of the model are those distributions in which one approximate factor  $\tilde{f}_i$  is replaced by the corresponding exact factor  $f_i$ . Namely,  $p^{\setminus j} \propto f_j \prod_{i \neq j} \tilde{f}_i$ . Therefore, PEP minimizes  $D_\alpha[p^{\setminus j}|q]$  for all  $j$ . In general, it is expected that a local minimization of the  $\alpha$ -divergence gives similar results to a global minimization while being a

much simpler problem [16].

To perform the local minimization of the  $\alpha$ -divergence PEP optimizes the following objective function:

$$\mathcal{L}(\phi, \{\theta_i\}_{i=1}^N) = \log Z_q - \log Z_{\text{prior}} + \frac{1}{\alpha} \sum_{i=1}^N \log \mathbb{E}_{q_\phi(\mathbf{w})} \left[ \left( \frac{p(y_i|\mathbf{w}, \mathbf{x}_i)}{\tilde{f}_i(\mathbf{w})} \right)^\alpha \right], \quad (21)$$

where  $Z_q$  is the normalization constant of  $q_\phi$ ,  $Z_{\text{prior}}$  is the normalization constant of the prior,  $\phi$  are the parameters of  $q$  and  $\{\theta_i\}_{i=1}^N$  are the parameters of the approximate factors  $\tilde{f}_i$ . In this case, we have assumed that the prior distribution need not be approximated and already belongs to the exponential family (*i.e.*, it is a Gaussian prior).

In practice, PEP solves the problem  $\max_\phi \min_{\{\theta_i\}_{i=1}^N} \mathcal{L}(\phi, \{\theta_i\}_{i=1}^N)$ , which is a very complicated task and requires a slow double loop algorithm [21]. Furthermore, PEP does not scale to big data and maintains an approximate factor associated to each likelihood factor resulting in a space complexity in  $\mathcal{O}(N)$ . When  $\alpha \rightarrow 0$  (21) converges to the lower bound of VI in (5) [16]. Therefore, a local minimization of the KL divergence employed in VI is equivalent to a global minimization.

#### 4.2. Black-box $\alpha$ -divergence Minimization

Black-box- $\alpha$  (BB- $\alpha$ ) is an improvement over the previous method, PEP, that addresses some of its limitations like the memory space requirements and also allows to make approximate inference on complicated probabilistic models [7]. For this, the PEP objective function is rewritten as:

$$\mathcal{L}(\phi) = \log Z_q - \log Z_{\text{prior}} + \frac{1}{\alpha} \sum_{i=1}^N \log \mathbb{E}_{q_\phi(\mathbf{w})} \left[ \left( \frac{p(y_i|\mathbf{w}, \mathbf{x}_i)}{\tilde{f}(\mathbf{w})} \right)^\alpha \right], \quad (22)$$

where now there is only one approximate factor  $\tilde{f}(\mathbf{w})$  that is replicated  $N$  times, one per each complicated likelihood factor. Therefore,  $q_\phi(\mathbf{w}) \propto \tilde{f}(\mathbf{w})^N p(\mathbf{w})$ . This solves the problem of having to store in memory the parameters of  $N$  factors. Furthermore, there is a one to one map between  $f(\mathbf{w})$  and  $q_\phi(\mathbf{w})$ . This

means that the max-min optimization problem of PEP is transformed into just a standard maximization problem (w.r.t to the parameters of  $q, \phi$ ), which can be solved using standard optimization techniques. Importantly, the expectations in (22) can be approximated via Monte Carlo sampling and the sum across the training data can be approximated using a mini-batch. The consequence is that BB- $\alpha$  scales to big datasets, as (22) can be optimized using stochastic techniques, and moreover, it can be applied to complicated probabilistic models (*e.g.*, Bayesian neural networks) in which the required expectations are intractable. Again, when  $\alpha \rightarrow 0$  (22) converges to the lower bound of VI in (5). When  $\alpha = 1$ , (22) is approximately equal to the objective optimized by Expectation Propagation [7]. A limitation of BB- $\alpha$  is, however, that the approximate distribution  $q$  is restricted to be inside the exponential family. This is because it must be written as the product of an approximate factor times the prior distribution. That is,  $q_\phi(\mathbf{w}) \propto \tilde{f}(\mathbf{w})^N p(\mathbf{w})$ . This is a major limitation that makes difficult using implicit models for  $q$ .

#### 4.3. Reparameterization of the Black-box- $\alpha$ Objective

In this section we describe the reparameterization for the general expression of the BB- $\alpha$  objective suggested in [19]. This reparameterization allows to approximately minimize  $\alpha$ -divergences with flexible distributions  $q$  such as the ones resulting from implicit models. To begin with, consider the following alternative expression for the BB- $\alpha$  objective:

$$\mathcal{L}_\alpha(\phi) = \frac{1}{\alpha} \sum_{i=1}^N \mathbb{E}_{q_\phi(\mathbf{w})} \left[ \left( \frac{p(y_i | \mathbf{x}_i, \mathbf{w}) p(\mathbf{w})^{1/N}}{q_\phi(\mathbf{w})^{1/N}} \right)^\alpha \right]. \quad (23)$$

In this expression we observe that the hypothesis that  $q_\phi(\mathbf{w}) \propto \tilde{f}^N(\mathbf{w}) p(\mathbf{w})$  is not required anymore (both  $Z_q$  and  $\tilde{f}(\mathbf{w})$  are removed from the expression) and  $q$  can be an arbitrary distribution. It is possible to show that (23) and (22) become equivalent if  $q$  belongs to the exponential family [19]. A difficulty is, however, that this expression requires the evaluation of the density  $q_\phi(\mathbf{w})$  which can be difficult to compute in practice.

To overcome the limitation described before, in [19], they reparametrize (23) using the so-called *cavity distribution*. That is, the distribution given by the ratio  $q_\phi/\tilde{f}^\alpha$ . If  $\tilde{q}_\phi(\mathbf{w})$  denotes a free-form cavity distribution, the posterior approximation  $q_\phi$  is given by:

$$q_\phi(\mathbf{w}) = \frac{1}{Z_q} \tilde{q}_\phi(\mathbf{w}) \left( \frac{\tilde{q}_\phi(\mathbf{w})}{p(\mathbf{w})} \right)^{\frac{\alpha}{N-\alpha}} \quad (24)$$

where we assume  $Z_q < +\infty$  is the normalizing constant to make  $q$  a valid distribution. When  $\alpha/N \rightarrow 0$  we have that  $q \rightarrow \tilde{q}$  (and  $Z_q \rightarrow 1$  by assumption), and this is the case either if we choose  $\alpha \rightarrow 0$  or  $N \rightarrow +\infty$ , given that  $\alpha$  grows sublinearly w.r.t  $N$ . See [19]. We rewrite now (23) in terms of  $\tilde{q}$  rather than  $q$ :

$$\begin{aligned} \mathcal{L}_\alpha(\phi) &= \frac{1}{\alpha} \sum_{i=1}^N \log \int \left( \frac{1}{Z_q} \tilde{q}_\phi(\mathbf{w}) \left( \frac{\tilde{q}_\phi(\mathbf{w})}{p(\mathbf{w})} \right)^{\frac{\alpha}{\alpha-N}} \right)^{1-\frac{\alpha}{N}} p(\mathbf{w})^{\frac{\alpha}{N}} p(y_i|\mathbf{w}, \mathbf{x}_i)^\alpha d\mathbf{w} \\ &= -\frac{N}{\alpha} \left( 1 - \frac{\alpha}{N} \right) \log \int \tilde{q}_\phi(\mathbf{w}) \left( \frac{\tilde{q}_\phi(\mathbf{w})}{p(\mathbf{w})} \right)^{\frac{\alpha}{N-\alpha}} d\mathbf{w} \\ &\quad + \frac{1}{\alpha} \sum_{i=1}^N \log \mathbb{E}_{\tilde{q}_\phi(\mathbf{w})} [p(y_i|\mathbf{x}_i, \mathbf{w})^\alpha] \\ &= \frac{1}{\alpha} \sum_{i=1}^N \log \mathbb{E}_{\tilde{q}_\phi(\mathbf{w})} [p(y_i|\mathbf{x}_i, \mathbf{w})^\alpha] - \mathbb{R}_\beta[\tilde{q}|p], \end{aligned} \quad (25)$$

where  $\beta = N/(N - \alpha)$  and  $\mathbb{R}_\beta[\tilde{q}|p]$  represents the *Rényi divergence* of order  $\beta$  [22], which is defined as

$$\mathbb{R}_\beta[q|p] = \frac{1}{\beta-1} \log \int \tilde{q}(\mathbf{w})^\beta p(\mathbf{w})^{1-\beta} d\mathbf{w}. \quad (26)$$

Importantly, when  $\alpha/N \rightarrow 0$  we recover  $q \rightarrow \tilde{q}$  and  $\mathcal{L}_\alpha(\phi)$  converges to the objective of VI. Moreover,  $\mathbb{R}_\beta[\tilde{q}|p] \rightarrow \text{KL}[\tilde{q}|p] = \text{KL}[q|p]$  if  $\mathbb{R}_\beta[\tilde{q}|p] < +\infty$  (which is true assuming  $Z_q < +\infty$ ) and  $\alpha/N \rightarrow 0$ . Therefore, for a constant  $\alpha$  that scales sub-linearly with  $N$ , we can make further approximations for the BB- $\alpha$

energy function described in (23), finally obtaining

$$\mathcal{L}_\alpha(\phi) \approx \frac{1}{\alpha} \sum_{i=1}^N \log \mathbb{E}_{q_\phi(\mathbf{w})} [p(y_i|\mathbf{x}_i, \mathbf{w})^\alpha] - \text{KL}[q_\phi(\mathbf{w})|p(\mathbf{w})], \quad (27)$$

which is the objective of our approach. Note that the expectations in (27) can be estimated via Monte Carlo sampling. In particular,  $\log \mathbb{E}_{q_\phi(\mathbf{w})} [p(y_i|\mathbf{x}_i, \mathbf{w})^\alpha] \approx \log [K^{-1} \sum_{k=1}^K p(y_i|\mathbf{x}_i, \mathbf{w}_k)^\alpha]$ , for  $K$  samples of  $\mathbf{w}$  drawn from  $q_\phi$ . Of course, this estimate is biased, as a consequence of the non-linearity of the  $\log(\cdot)$  function, however, the bias is reduced with  $K$ . Furthermore, we expect a similar behavior as in standard BB- $\alpha$ , in which the bias has been shown to be very small even for  $K = 10$  samples. See [7] for further details.

The objective in (27) has been obtained under some conditions that need not be true in practice, *e.g.*,  $\alpha/N \rightarrow 0$ . Nevertheless, it is much simpler to estimate and optimize than the one in (23). It is also similar to the objective functions found in the deep learning bibliography (*i.e.*, a loss function plus some regularizer, *i.e.*, the KL divergence), but it still maintains the qualities of an approximate Bayesian inference algorithm. Importantly, (27) allows for implicit models for  $q_\phi$ . The only term that is difficult to approximate is  $\text{KL}[q_\phi(\mathbf{w})|p(\mathbf{w})]$ . However, the approach described in Section 2.2 can be used for that purpose. By changing the  $\alpha$  parameter of the method we will be able to interpolate between AVB ( $\alpha \rightarrow 0$ ) and an EP like algorithm ( $\alpha = 1$ ). Note that when  $\alpha \rightarrow 0$ , (27) is expected to focus on reducing the training error since the factor  $\alpha^{-1} \log \mathbb{E}_{q_\phi(\mathbf{w})} [p(y_i|\mathbf{x}_i, \mathbf{w})^\alpha]$  will converge to  $\mathbb{E}_{q_\phi(\mathbf{w})} [\log p(y_i|\mathbf{x}_i, \mathbf{w})]$ , with  $p(y_i|\mathbf{x}_i, \mathbf{w})$  typically a Gaussian distribution with mean given by the output of the neural network and noise variance  $\sigma^2$ . By contrast, when  $\alpha = 1$ , (27) will consider the training log-likelihood. Intermediate values of  $\alpha$  will trade-off between these two tasks, which may lead to better generalization properties.

With respect to the specific details of the proposed approach, it is analogous to the one presented in AVB [10], and therefore will consider three networks: An implicit model for  $q_\phi$ , which takes as input Gaussian noise and outputs neural

network weight samples  $\mathbf{w}$  from the approximated weights posterior distribution; a discriminator, which estimates the KL term present in (27) as done in [10]; and finally the main network, that uses the samples of the weights generated previously to evaluate the factor  $p(y_i|\mathbf{x}_i, \mathbf{w})$ . The whole system is optimized all together. Furthermore, any potential hyper-parameter (*e.g.*, the prior variance  $\sigma_0^2$  or the output noise variance  $\sigma^2$ ) is tuned simply by maximizing (27).

Finally, as a last remark concerning the implementation of the proposed method, we have also included as trainable parameters both the mean and variances of the Gaussian noise which is used as input in the generator network,  $\epsilon \sim \mathcal{N}(\boldsymbol{\mu}_{\text{noise}}, \boldsymbol{\Sigma}_{\text{noise}})$ , with  $\boldsymbol{\Sigma}_{\text{noise}}$  a diagonal matrix. This allows for a more expressive implicit model for  $q_\phi$ , which is expected to reproduce to a higher degree of accuracy the original posterior distribution of the model parameters (neural network weights).

#### 4.3.1. Annealing Factor

When optimizing the objective of the proposed method, it may converge to a bad local optimum in which the method pays too much attention to the KL term and fails to explain the observed data. Therefore, it is convenient to train the method in such a way that we try to avoid local optima. For this, we incorporated the technique described in [23].

With the goal described, we define a *warm-up* period for which we will train our model *turning on progressively* the KL term in the objective function. We do this by changing slightly the original formulation of (27) to introduce an extra *annealing parameter*  $\beta$ . That is,

$$\mathcal{L}_\alpha(\phi) \simeq \frac{1}{\alpha} \sum_{i=1}^N \log \mathbb{E}_{q_\phi(\mathbf{w})} [p(y_i|\mathbf{x}_i, \mathbf{w})^\alpha] - \beta \text{KL}[q_\phi(\mathbf{w})|p(\mathbf{w})], \quad (28)$$

where  $\beta$  starts being equal to 0 and grows linearly to 1 during a certain number of epochs. If it is not stated otherwise, the number of warm-up epochs is selected to be the 10% of the total epochs assigned for training the algorithm in a given dataset (extracted from the UCI repository). We have observed that

this significantly improves the results of the proposed method. In the case of the synthetic problems, the warm up period is set to 500 epochs from a total number of 3000 epochs. In the experiments with big data we have not included the annealing factor since it has not been observed to be beneficial.

## 5. Related Work

Obtaining the uncertainty in the predictions of machine learning algorithms is a widely spread problem. Originally, this problem has been addressed either by sampling-based methods or by optimization-based methods [13]. In sampling-based methods, the posterior distribution is approximated by drawing samples from the exact posterior to then use these for inference and prediction. For this, a Markov chain is run, whose stationary distribution coincides with the target distribution. On the other hand, optimization-based methods introduce an approximate distribution  $q$  whose parameters are adjusted to match the exact posterior through the optimization of a certain objective.

Each of the approaches described has advantages and disadvantages. Sampling methods can be unbiased only asymptotically, and moreover they can be highly computationally expensive since the Markov chain has to be run for long time in practice. Similarly, optimization-based techniques are usually limited by the definition of the approximating distribution, which is often parametric, and therefore they may lack expressiveness. Two examples of these methods are Markov chain Monte Carlo (MCMC) in the case of sampling-based methods [24, 25, 5], and variational inference (VI) or expectation propagation (EP) in the case of optimization-based methods [18, 26, 8, 14]. The method proposed here alleviates some of the problems of these two techniques. Specifically, it allows for flexible approximate distributions and it also scales to large datasets.

Most modern techniques for approximate inference take advantage of the speed of optimization-based methods and try to preserve the flexibility of sampling-based methods with the goal of obtaining the best results possible in terms of computational cost and accuracy of the approximation. There are, however,

many different ways of combining both approaches, which is showcased by the wide variety of methods proposed. In this section we review some of them. Nevertheless, almost all of them rely on optimizing the KL divergence between  $q$  and the target distribution. The approach proposed by us is more general and can minimize a collection of divergences known as the  $\alpha$ -divergence, which includes also the KL divergence as a particular case.

One example is the work in [27], where it is described how to estimate the gradient of the VI objective when using an implicit model for the approximate distribution  $q$ . For this, the method described in that work proposes a complex combination of Markov chain Monte Carlo methods and VI. While this approach seems promising, its implementation is very complicated since it relies on running an inner Markov chain inside of the optimization process of the approximate distribution  $q$ . This Markov chain has also parameters that need to be correctly adjusted and that may depend on the probabilistic model.

Another approach that allows for flexible approximate distributions  $q$  within the context of VI is normalizing flows (NF) [9]. In NF one starts with a simple parametric approximate distribution  $q$  whose samples are modified using parametric non-linear invertible transformations. If these transformations are chosen carefully, the p.d.f. of the resulting distribution can be evaluated in closed form, avoiding the problems arising from the use of implicit models for  $q$ . The problem of NF is that the family of transformations that can be used is limited, which may constrain the flexibility of the approximate distribution  $q$ .

*Stein Variational Gradient Descent*, proposed in [11], is a general VI method that consists in transforming a set of *particles* to match the exact posterior distribution. The results obtained are shown to be competitive with other state-of-the-art methods, but the main drawback here is that there is a computational bottleneck on the number of particles that need to be stored to accurately represent the posterior distribution. More precisely, this method lacks a way to generate samples from the approximate distribution  $q$ . The number of samples is fixed initially, and these are optimized by the method.

The work in [12] combines VI and MCMC methods to obtain flexible ap-

proximate posterior distributions. The key concept is to use a Markov chain as the approximate distribution  $q$  in VI. The parameters of this chain can then be adjusted to match as close as possible the target distribution in terms of the KL divergence. This is an interesting idea. However, it is also limited by the difficulty of evaluating the p.d.f. of the approximate distribution. This is solved in [12] by learning a backward model, that infers the p.d.f. of the initial state of the Markov chain given the generated samples. Learning this backward model accurately is difficult, which limits the practical applicability of the method.

Another approach used for approximate inference in the context of neural networks is Probabilistic Back-propagation [6]. This method computes a forward propagation of probabilities through the neural network to then do back-propagation of the gradients. Although it has been proven to be a fast approach with high performance, it is limited by the expressiveness of the posterior approximation. In particular, the approximate distribution is restricted to be Gaussian. This means that this method will suffer from strong approximation bias. The same applies to a standard application of VI in the context of Bayesian neural networks [8].

The minimization of  $\alpha$ -divergences in the context of Bayesian neural networks has also been addressed in [6]. In that work it is described Black-box- $\alpha$ , a method for approximate inference that allows for very complex probabilistic models and that is efficient and allows for big datasets. The main limitation is, however, that the approximate distribution  $q$  must belong to the exponential family. That is, the approximate distribution has to be Gaussian, and hence, this method will also suffer from approximation bias. Therefore, Black-box- $\alpha$  is expected to be sub-optimal when compared to the method proposed in this paper, which allows for implicit models in the approximate distribution  $q$ .

The minimization of  $\alpha$ -divergences has also been explored in the context of dropout in [19]. That work considers the same objective as the one optimized by our approach in Section 4.3. The difference is that the approximate distribution considered by the authors of that work is limited to the approximate posterior distribution of dropout. This distribution is given by the mixture of two points

of probability mass, *i.e.*, two delta functions, one of which is located at the origin [28]. The flexibility of this approximate distribution is hence very limited. By contrast, the method we propose allows for implicit approximate distributions  $q$  and therefore is expected to give superior results.

Finally, a closely related method to ours is the one described in [10]. This method, Adversarial Variational Bayes (AVB), allows to carry out Variational Inference with implicit models as the approximate distribution  $q$ . For this, in that work it is proposed to train a discriminator whose output can be used to estimate the KL divergence between the approximate distribution  $q$  and the prior. A limitation of [10] is that the method described there is restricted to minimize the KL divergence between the approximate and the target distribution. Our approach, by contrast, can optimize the more general  $\alpha$ -divergence, which includes the KL divergence as a particular case. Therefore, by changing the  $\alpha$  parameter our method can potentially obtain better results than AVB. This hypothesis is confirmed by the experiments of the next section.

## 6. Experiments

To analyze and evaluate the performance of the proposed approach, *i.e.*, Adversarial  $\alpha$ -divergence Minimization (AADM), we have carried out extensive experiments, both in synthetic data and on common UCI datasets [29]. Furthermore, we have compared results with previously existing methods such as VI, using a factorizing Gaussian as the approximate distribution, and AVB, which is a particular case of AADM which optimizes the KL divergence. That is, AADM should give the same results as AVB for  $\alpha \rightarrow 0$ . In these experiments we have also analyzed performance versus computational cost of each method on larger datasets with up to 2 million data points.

The method AADM employed in our experiments consists in the previously described three-network system. In particular, the structure we have considered for AADM (and also AVB) is the following one: The generator network takes as an input a 100-dimensional Gaussian noise sample, with adjustable mean and

diagonal covariance parameters, and passes it through 2 layers of 50 non-linear units each, outputting a sample of the weights  $\mathbf{w}$ . We generate 10 samples for the weights when training, and 50 samples to approximate the predictive distribution when testing. Similarly, the discriminator takes these samples of the weights (as well as samples from the auxiliary distribution described in Section 2.3) and passes them through 2 layers of 50 non-linear units each to compute  $T_\omega(\mathbf{w})$ . Finally, the main network (*i.e.*, the model whose weights we are inferring) also consists of a 2 layer system with 50 units per layer as well. This network uses the sampled weights and the original data as input to estimate the AADM objective  $\mathcal{L}_\alpha(\phi)$ . Note that although the network size employed in our experiments is small, it is similar to the network size considered in recent related works [6, 19].

The structure described is maintained throughout all the experiments, and remains the same if it is not stated otherwise for each specific case. The number of training epochs and the presence (or absence) of a warm-up period depends on the dataset being used, and therefore is specified in each experiment. All non-linear units are leaky RELU units. The code implementing the proposed approach is available online at <https://github.com/simonrsantana/AADM>. All methods have been trained using stochastic optimization via ADAM [30]. The learning rate for updating the parameters of the discriminator is set to the default value in ADAM, *i.e.*,  $10^{-3}$ . The learning rate for updating the implicit model for  $q_\phi$  (*i.e.*, the generator) and the model hyper-parameters (which includes the variance of the output noise and the prior) is set to  $10^{-4}$ . Apart from this, we use the default parameter values in ADAM. The mini-batch size used is described in each experiment.

### 6.1. Synthetic Experiments

In order to analyze the behavior of the proposed method we evaluate the AADM on two simple regression problems extracted from [31]. More precisely, we generate two different *toy datasets*. The first one involving a heteroscedastic predictive distribution, and the second one involving a bimodal predictive

distribution.

The structure of the system employed is the one described previously. We train this system for 3000 epochs, using the first 500 epochs as the warm-up period. We repeat the experiments for different values of alpha in the  $(0, 1]$ . The first dataset is generated taking  $x$  uniformly distributed in the interval  $[-4, 4]$  and  $y$  is obtained as  $y = 7 \sin x + 3|\cos(x/2)|\epsilon$ , where  $\epsilon$  is normally-distributed and independent of  $x$ , *i.e.*,  $\epsilon \sim \mathcal{N}(0, 1)$ . Note that this dataset involves input dependent noise. The second dataset uses  $x$  uniformly distributed in the interval  $[-2, 2]$  and  $y = 10 \sin x + \epsilon$  with probability 0.5 and  $y = 10 \cos x + \epsilon$  otherwise. The distribution of  $\epsilon$  is the same as in the first dataset. note that this other dataset involves a bimodal predictive distribution. We use 1000 data instances for training and the mini-batch size is set to 10.

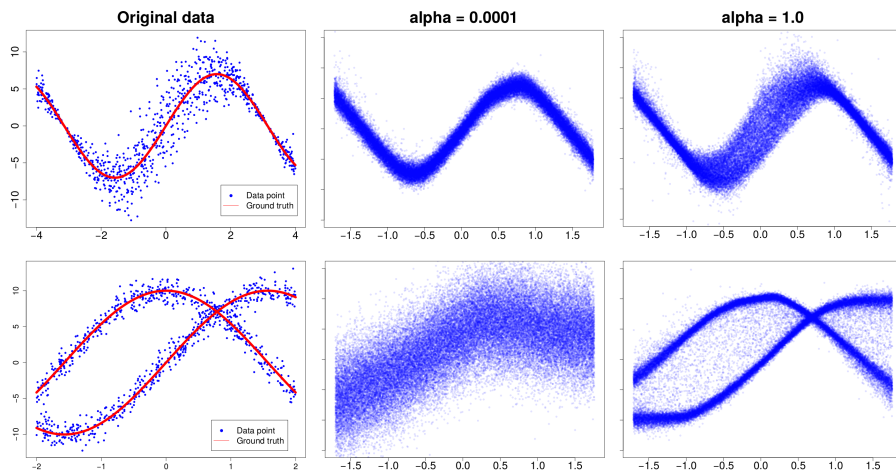


Figure 2: Results for the toy problems. The blue points on the left represent the original training data and the ground truth (red lines). In the middle, predictions generated with  $\alpha \approx 0$  (*i.e.* regular AVB), and in the right side are the predictions with  $\alpha = 1.0$ .

The results obtained in the synthetic problems described are represented in Figure 2. The top figures correspond to the problem involving the heteroscedastic noise and the bottom ones to the problem with a bimodal predictive distribution. On the left of the figure we show the original data we used to train

Table 1: Log-likelihood and error results for AADM with  $\alpha = 10^{-4}$  and  $\alpha = 1.0$  in both toy experiments.

$\alpha$	Bimodal		Heteroscedastic	
	Log-likelihood	RMSE	Log-likelihood	RMSE
$10^{-4}$	3.05	5.10	2.08	1.91
1.0	2.17	5.18	1.91	1.94

AADM. In these plots, the red lines represent the *ground truth* for each dataset and the blue points are the actual samples we used as training data. The middle and right columns show samples from the predictive distribution of a neural network trained using AADM, for  $\alpha = 10^{-4}$  and  $\alpha = 1$ , respectively. The results obtained for  $\alpha = 10^{-4}$  are expected to be equal to those of AVB. As can be noticed, a low value of alpha is unable to reproduce the complex structure of the data, losing main qualities such as the heteroscedastic additive noise in the first task and the bimodality of the predictive distribution in the second task. However, both of them are recovered with accuracy when alpha is higher, which is showcased by the results obtained when  $\alpha = 1$ .

The results obtained in these experiments, although synthetic, already show that choosing one value of  $\alpha$  or another, for the divergence that is approximately optimized in AADM can significantly change the results obtained. In particular, when  $\alpha = 10^{-4}$  we can observe that the predictive distribution that is obtained (after fitting the posterior approximation) focuses more on minimizing the squared error and less on the log-likelihood of the data. By contrast, when  $\alpha = 1.0$ , the predictive distribution plays a closer attention to the log-likelihood of the data, and can hence obtain a more accurate predictive distribution. As can be seen in Table 1, although the squared error obtained when  $\alpha = 10^{-4}$  and  $\alpha = 1.0$  is very similar, the test log-likelihood obtained when  $\alpha = 1.0$  is much better since this value of  $\alpha$  produces more accurate predictive distributions.

Finally, other values of  $\alpha$  give similar results (not shown here). In particular, for  $\alpha < 0.5$  similar results to those of  $\alpha = 10^{-4}$  are obtained. By contrast, when  $\alpha > 0.5$  similar results to those of  $\alpha = 1.0$  are obtained (that is, only if the

Table 2: Characteristics of the UCI datasets used in the experiments.

<b>Dataset</b>	<b>Instances</b>	<b>Attributes</b>	<b>Epochs</b>
Boston	506	13	2000
Concrete	1,030	8	2000
Energy Efficiency	768	8	2000
Kin8nm	8,192	8	400
Naval	11,934	16	400
Combined Cycle Power Plant	9,568	4	250
Wine	1,599	11	2000
Yatch	308	6	2000

training procedure is carried out carefully to avoid bad local optima).

### 6.2. Experiments on UCI Datasets

To analyze in more detail the results of the proposed method, AADM, we have considered eight UCI datasets [29] that are widely spread for regression [6]. The characteristics of these datasets are displayed in Table 2. Each dataset has a different size, and in order to train the different methods until convergence we have employed a different number of epochs in each case. The number of epochs selected is presented finally in Table 2. Note that, even though there are differences in the epochs employed for training, all of the datasets share the same model structure, which is the general one described at the beginning of this section. In all these experiments we employ the first 10% of the total training epochs for *warming-up* before the KL term is completely turned on as in [23]. Moreover, the batch size is set to be 10 data points, and sampling-wise, we perform 10 samples in the training procedure and 100 for testing. We split the datasets in a 90%-10% for training/testing. The results reported are averages over 20 different random splits of the datasets into training and testing.

We compare the results of AADM with VI using a factorizing Gaussian as the posterior approximation and with regular AVB (which should be the same as our algorithm when  $\alpha \rightarrow 0$ ). Both for VI and AVB we employ a the same two-layered system with 50 units per layer, and in AVB we use the same structure. To make fair comparisons we also perform the same warm-up period for both

AVB and VI as we use in our method. Therefore only after the first 10% of the total number of epochs, the KL term is completely activated in the objective function.

The average performance of each method on each dataset, in terms of the test log-likelihood, is displayed Figure 3. We observe that values of  $\alpha$  that are different to 0 that usually outperform both regular AVB and VI in terms of this metric (the higher the values the better). From these figures, it seems that higher values of  $\alpha$  often lead to better predictive distributions in terms of the test log-likelihood, probably as a consequence of being able to better recover the real posterior distribution. The values obtained are similar and often better than those of other state of the art methods [6]. Each of the values shown represent the mean performance of a certain method across the 20 different splits of each dataset, which are averaged afterwards here. Importantly, we observe that standard VI is almost always outperformed by the two techniques that allow for implicit models in the posterior approximation  $q$ . Namely, AVB and AADM. This points out the benefits of using an implicit model for the approximate distribution  $q$ . Moreover, AVG and AADM give almost the same results when  $\alpha \approx 0$ , which confirms the correctness of our implementation.

The average results obtained for each method on each dataset, in terms of the root mean squared error (RMSE) are displayed in Figure 4. We can see that the proposed approach, AADM, also obtains better results than VI. In this case, nonetheless, different  $\alpha$  values do not actually improve much over the basic results of AVB, and in general we can see that lower values for  $\alpha$  are actually better to obtaining a good performance in terms of this metric (here, the lower in the graphs the better the performance). This seems to indicate that one should choose a value for  $\alpha$  that is different, depending on the metric they are most interested in. These results are consistent in the sense that, as pointed out previously, values of  $\alpha$  close to zero actually lead to the objective that is optimized in AVB and VI, which pays more attention to the training RMSE, in the case of regression problems with Gaussian noise. By contrast, values of  $\alpha$  closer to one, pay more attention to the log-likelihood of the training data.

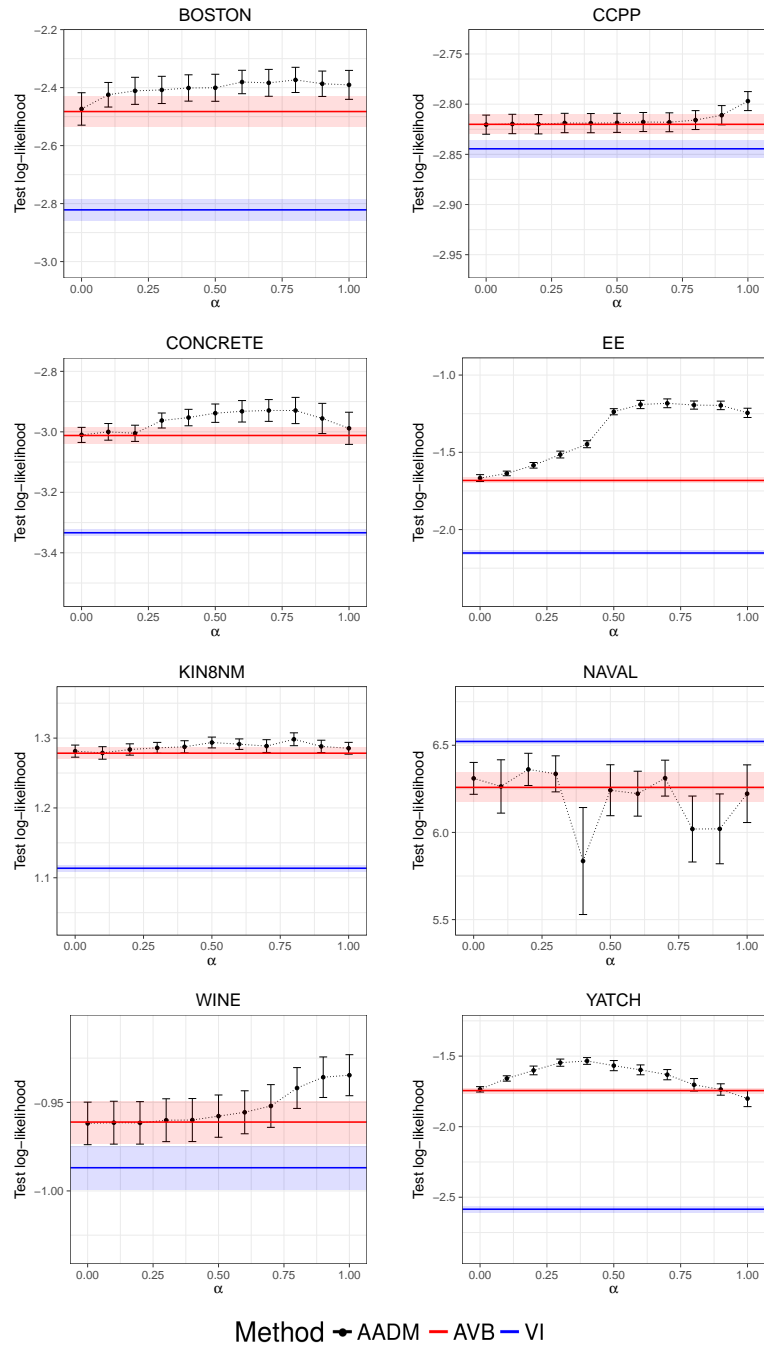


Figure 3: Average results in terms of the test log-likelihood for the different UCI datasets and methods compared. Black represents the performance for our method, AADM, for different values of  $\alpha$ . Red is the performance of AVB. VI is presented in blue. Best seen in color.

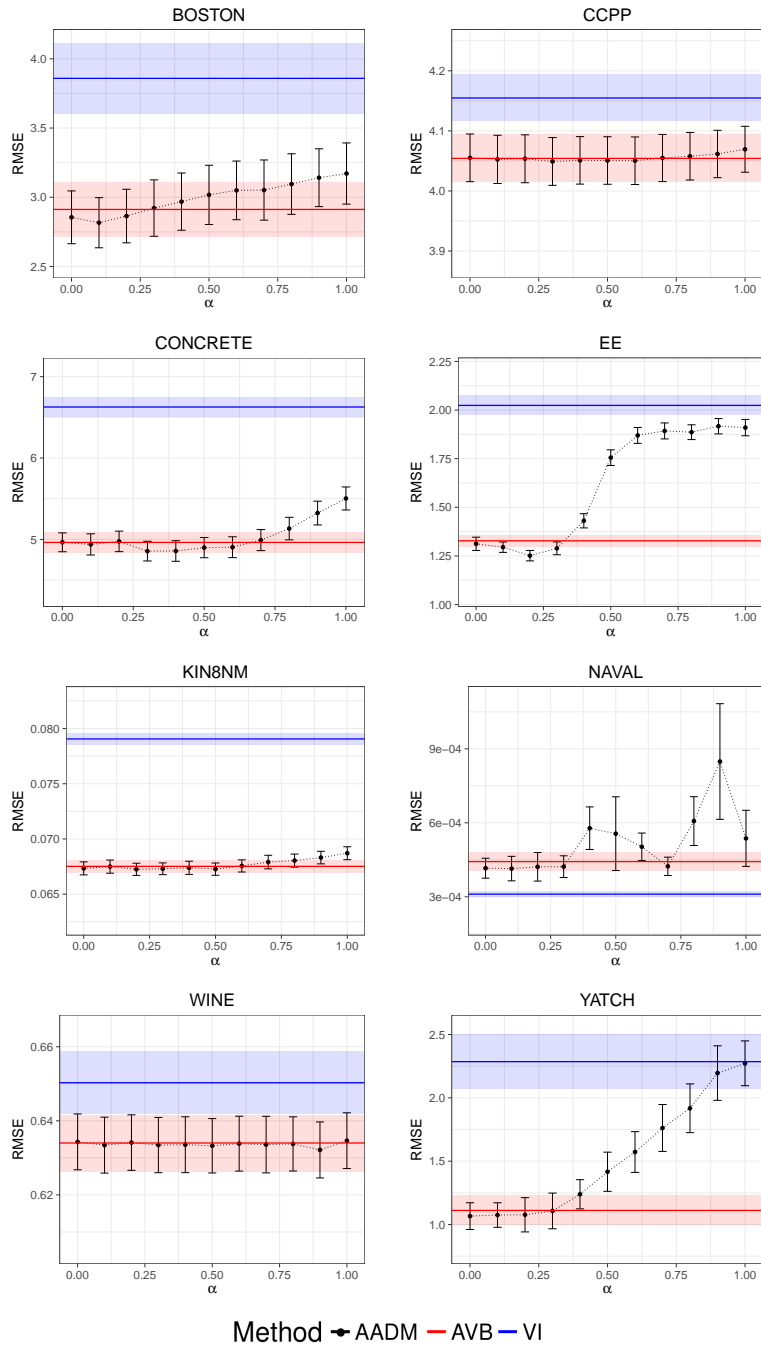


Figure 4: Average results in terms of the root mean squared error for the different UCI datasets and methods compared. Black represents the performance for our method, AADM, for different values of  $\alpha$ . Red is the performance of AVB. VI is presented in blue. Best seen in color.

### 6.2.1. Average Rank Results on the UCI Datasets

To get an overall idea about the performance of AADM, for each value of  $\alpha$ , on the previous experiments we have proceeded as follows: We have ranked the performance AADM for each  $\alpha$  value (*i.e.*, rank 1 means that value of  $\alpha$  gives the best result, rank 2 means that it gives the second best results, etc.). Then, we have computed the average rank over all the train / test splits of the datasets, and have calculated the standard deviation in each case. Figure 5 shows the results obtained for the RMSE and test log-likelihood.

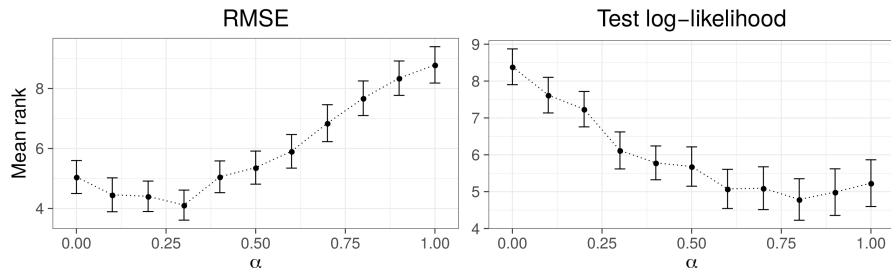


Figure 5: Average rank (the lower the better) for AADM and each value of  $\alpha$  in terms of the RMSE (left) and the test log-likelihood (right) across all the UCI datasets and splits.

The results obtained are displayed in Figure 5. This figure confirms that medium values for alpha usually present a better performance than the extremes (*i.e.*,  $\alpha \approx 0$  or  $\alpha = 1$ ), for both the RMSE and the test log-likelihood metrics. Furthermore, in the case of the test log-likelihood, higher values of  $\alpha$  provide a better recovery of the predictive distribution (and hence also the posterior), as indicated by the test log-likelihood. In spite of this, lower values of  $\alpha$  tend to perform better in terms of the RMSE. Again, this behavior can be explained by paying attention to the form the objective function optimized in both extremes. The VI objective is recovered when  $\alpha \rightarrow 0$ . This objective gives higher importance to the squared errors. By contrast, a similar objective function to the one of Expectation Propagation is obtained when  $\alpha = 1$ . This objective includes terms that involve the log-likelihood of the training data. The

main conclusion from this analysis is that the optimal value for  $\alpha$  depends on the metric we are considering, and that intermediate values of  $\alpha$ , different from 0 or 1 are expected to provide the best results.

### 6.3. Experiments on Big Datasets

To evaluate the performance of the proposed method on large datasets, we have carried out additional experiments considering two datasets: *Airlines Delay*, and *Year Prediction MSD*. *Airlines Delay* contains information about all commercial flights in the USA from January 2008 to April 2008 [32]. The task of interest is to predict the delay in minutes of a flight based on 8 attributes: age of the aircraft, distance that needs to be covered, air-time, departure time, arrival time, day of the week, day of the month and month. This is hence a very noisy dataset. After removing instances with missing values 2, 127, 068 instances remain. From these, 10,000 are used for testing and the rest are used for training. *Year Prediction MSD* is publicly accessible on the UCI repository [29]. This dataset has 515,345 data instances and 90 attributes. Again, we use 10,000 for testing and the rest of the data are used for training. In these experiments the mini-batch size has been set to 100 and we have not used the warm-up annealing scheme that deactivates the KL term in the objective of each method during the initial training iterations. For each method, we measured the performance in the test set, in terms of the RMSE and the test log-likelihood, as a function of the training time.

The results obtained for each method on the Airlines dataset are displayed in Figure 6. In this figure dashed lines represent other methods, the black being AVB and the blue VI. Solid lines represent our method, AADM, for different values of alpha. The figure shows that AADM obtains better results than AVB and VI in terms of the test log-likelihood when  $\alpha$  approaches 1. When  $\alpha$  is closer to 0, AADM, gives similar results to those of AVB and VI in the long term. The performance of our method w.r.t. the computational time is comparable to that of AVB. In terms of RMSE, however, large values of  $\alpha$  seem to exhibit a more unstable behavior and in general give worse results. This is probably a

consequence of this dataset being very noisy.

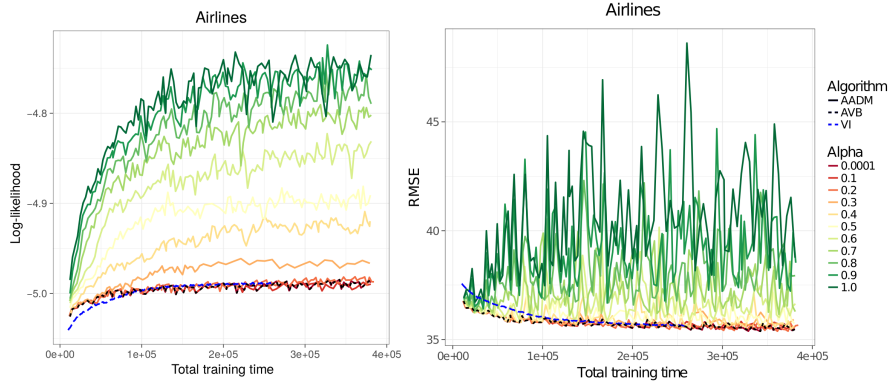


Figure 6: Performance as a function of the computational time in the Airlines dataset for each method. We report both in test log-likelihood (left) and the RMSE (right). The dashed blue line corresponds to the method VI, the dashed black line to AVB, and other solid lines represent our method, AADM, for different values of alpha. Best seen in color.

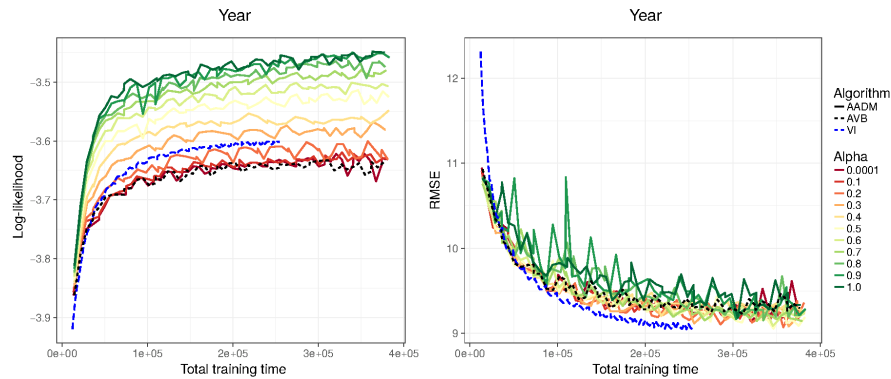


Figure 7: Performance as a function of the computational time in the Year dataset for each method. We report both in test log-likelihood (left) and the RMSE (right). The dashed blue line corresponds to the method VI, the dashed black line to AVB, and other solid lines represent our method, AADM, for different values of alpha. Best seen in color.

The results obtained for each method on the Year dataset are displayed in Figure 7. Again, in this figure dashed lines represent other methods, the

black being AVB and the blue VI. Solid lines represent our method, AADM, for different values of alpha. As in the previous dataset, AADM obtains better results than AVB and VI in terms of the test log-likelihood when  $\alpha$  approaches 1. When  $\alpha$  is closer to 0, AADM, gives similar results to those of AVB and VI. In terms of RMSE, lower values of  $\alpha$  seems to give also the best results. However, in this case higher values of  $\alpha$  do not seem to give significantly worse results in terms of this metric.

## 7. Conclusions

An estimate of the uncertainty in the predictions made by machine learning algorithms like neural networks is of paramount importance in some specific applications. This estimate can be obtained by following a Bayesian approach. More precisely, the posterior distribution captures which model parameters (neural network weights) are compatible with the observed data. The posterior distribution can then be used to compute a predictive distribution that summarizes the uncertainty in the predictions made. A difficulty, however, is that computing the posterior distribution is intractable and one has to resort to approximate methods in practice.

In this paper we have described a general method for approximate Bayesian inference. This method is known as Adversarial  $\alpha$ -divergence Minimization (AADM) and it allows to tune an approximate posterior distribution by approximately minimizing the  $\alpha$ -divergence between this distribution and the posterior. The  $\alpha$ -divergence generalizes the KL divergence, commonly used to perform approximate inference. AADM also allows to account for implicit models in the approximate posterior distribution. Implicit models allow to specify a probability distribution simply as some non-linear transformation of random input noise. If the non-linear transformation is flexible enough, this leads to a very flexible model. A drawback of implicit models is, however, that one cannot evaluate the p.d.f. of the resulting distribution, which is required for approximate inference. We overcome this problem by following the approach of [10]. More

precisely, we learn a discriminative model that estimates the log-ratio between the p.d.f. of the implicit model and a much simpler distribution (*i.e.*, a Gaussian distribution).

The proposed method, AADM, has been evaluated on several experiments and compared to other methods for approximate inference such as Variational Inference (VI) with a factorizing Gaussian as the approximate distribution, and Adversarial Variational Bayes (AVB) [10]. The experiments carried out, involving approximate inference with Bayesian neural networks, indicate that implicit models almost always provide better results than a factorizing Gaussian. Moreover, the minimization of  $\alpha$ -divergences seems to provide sometimes better results than the plain minimization of the KL divergence, as done by VI and AVB. In particular, values of  $\alpha$  that are close, but not exactly equal to 1 seem to provide better predictive distributions in terms of the test log-likelihood. By contrast, in terms of the root mean squared error (RMSE) one should choose values of  $\alpha$  that are close to, but not exactly equal to zero. We conclude therefore, that one can obtain better results in terms of the test log-likelihood and the RMSE by employing the proposed method, AADM, and by choosing a value of  $\alpha$  that may depend on the specific performance metric we are interested in.

### **Acknowledgements**

Simón Rodríguez acknowledges the Spanish Ministry of Economy for the FPI SEV-2015-0554-16-4 Ph.D. scholarship. The authors gratefully acknowledge the use of the facilities of Centro de Computación Científica (CCC) at Universidad Autónoma de Madrid. Daniel Hernández-Lobato also acknowledges financial support from Spanish Plan Nacional I+D+i, grants TIN2016-76406-P and TEC2016-81900-REDT.

## References

## References

- [1] Y. LeCun, Y. Bengio, G. Hinton, Deep learning, *Nature* 521 (2015) 436–444.
- [2] A. Krizhevsky, I. Sutskever, G. E. Hinton, Imagenet classification with deep convolutional neural networks, in: *Advances in Neural Information Processing Systems*, 2012, pp. 1097–1105.
- [3] S. Hochreiter, J. Schmidhuber, Long short-term memory, *Neural computation* 9 (1997) 1735–1780.
- [4] Y. Gal, Uncertainty in deep learning, Ph.D. thesis, PhD thesis, University of Cambridge (2016).
- [5] R. M. Neal, *Bayesian learning for neural networks*, Vol. 118, Springer Science & Business Media, 2012.
- [6] J. M. Hernández-Lobato, R. P. Adams, Probabilistic backpropagation for scalable learning of Bayesian neural networks, in: *International Conference on Machine Learning*, 2015, pp. 1861–1869.
- [7] J. M. Hernández-Lobato, Y. Li, M. Rowland, D. Hernández-Lobato, T. D. Bui, R. E. Turner, Black-box  $\alpha$ -divergence minimization (2016) 1511–1520.
- [8] A. Graves, Practical variational inference for neural networks, in: *Advances in neural information processing systems*, 2011, pp. 2348–2356.
- [9] D. J. Rezende, S. Mohamed, Variational inference with normalizing flows, in: *International Conference on Machine Learning*, 2016, pp. 1530–1538.
- [10] L. Mescheder, S. Nowozin, A. Geiger, Adversarial variational bayes: Unifying variational autoencoders and generative adversarial networks, in: *International Conference on Machine Learning*, 2017, pp. 2391–2400.

- [11] Q. Liu, D. Wang, Stein variational gradient descent: A general purpose Bayesian inference algorithm, in: *Advances In Neural Information Processing Systems*, 2016, pp. 2378–2386.
- [12] T. Salimans, D. Kingma, M. Welling, Markov chain Monte Carlo and variational inference: Bridging the gap, in: *International Conference on Machine Learning*, 2015, pp. 1218–1226.
- [13] Y. Li, Q. Liu, Wild variational approximations, in: *NIPS workshop on advances in approximate Bayesian inference*, 2016.
- [14] M. J. Beal, Variational algorithms for approximate Bayesian inference, Ph.D. thesis (2003).
- [15] S. Amari, *Differential-geometrical methods in statistics*, Vol. 28, Springer Science & Business Media, 2012.
- [16] T. Minka, Divergence measures and message passing, Tech. rep., Technical report, Microsoft Research (2005).
- [17] B. J. Frey, R. Patrascu, T. Jaakkola, J. Moran, Sequentially fitting “inclusive” trees for inference in noisy-or networks, in: *Advances in Neural Information Processing Systems*, 2001, pp. 493–499.
- [18] T. P. Minka, Expectation propagation for approximate bayesian inference, in: *Uncertainty in Artificial Intelligence*, 2001, pp. 362–369.
- [19] Y. Li, Y. Gal, Dropout inference in bayesian neural networks with alpha-divergences, in: *International Conference on Machine Learning*, 2017, pp. 2052–2061.
- [20] T. P. Minka, Power ep, Tech. rep., Technical report, Microsoft Research, Cambridge (2004).
- [21] T. Heskes, O. Zoeter, Expectation propagation for approximate inference in dynamic Bayesian networks, in: *Uncertainty in Artificial Intelligence*, 2002, pp. 216–223.

- [22] A. Rényi, On measures of entropy and information, in: Fourth Berkeley Symposium on Mathematical Statistics and Probability, Vol. 1, 1961, pp. 547–561.
- [23] C. K. Sønderby, T. Raiko, L. Maaløe, S. K. Sønderby, O. Winther, Ladder variational autoencoders, in: Advances in neural information processing systems, 2016, pp. 3738–3746.
- [24] S. Duane, A. D. Kennedy, B. J. Pendleton, D. Roweth, Hybrid Monte Carlo, *Physics letters B* 195 (1987) 216–222.
- [25] R. M. Neal, MCMC using Hamiltonian dynamics, in: Handbook of Markov chain Monte Carlo, 2011, pp. 113–162.
- [26] M. I. Jordan, Z. Ghahramani, T. S. Jaakkola, L. K. Saul, An introduction to variational methods for graphical models, *Machine learning* 37 (1999) 183–233.
- [27] M. K. Titsias, F. J. R. Ruiz, Unbiased implicit variational inference, in: Artificial Intelligence and Statistics, 2019, pp. 167–176.
- [28] Y. Gal, Z. Ghahramani, Dropout as a Bayesian approximation: Representing model uncertainty in deep learning, in: International Conference on Machine Learning, 2016, pp. 1050–1059.
- [29] D. Dua, C. Graff, UCI machine learning repository (2017).  
URL <http://archive.ics.uci.edu/ml>
- [30] D. P. Kingma, J. Ba, ADAM: a method for stochastic optimization, in: International Conference on Learning Representations, 2015, pp. 1–15.
- [31] S. Depeweg, J. M. Hernández-Lobato, F. Doshi-Velez, S. Udluft, Learning and policy search in stochastic dynamical systems with Bayesian neural networks, arXiv preprint arXiv:1605.07127.
- [32] J. Hensman, N. Fusi, N. D. Lawrence, Gaussian processes for big data, in: Uncertainty in Artificial Intelligence, 2013, pp. 282–290.